Accepted Manuscript

A micromechanical study of stress concentrations in composites

Hossein Ghayoor, Suong V. Hoa, Catharine C. Marsden

PII: S1359-8368(16)33114-6

DOI: 10.1016/j.compositesb.2017.09.009

Reference: JCOMB 5254

To appear in: *Composites Part B*

Received Date: 15 December 2016

Revised Date: 31 July 2017

Accepted Date: 4 September 2017

Please cite this article as: Ghayoor H, Hoa SV, Marsden CC, A micromechanical study of stress concentrations in composites, *Composites Part B* (2017), doi: 10.1016/j.compositesb.2017.09.009.

A Micromechanical Study of Stress Concentrations in Composites

Hossein Ghayoor*, Suong V. Hoa, Catharine C. Marsden

Concordia Center for Composites (CONCOM), Department of Mechanical and Industrial Engineering, Concordia University, Montreal, Quebec, Canada H3G 1M8

Abstract

Random and periodic representations of composite microstructures are inherently different both in terms of the resultant range of stresses that each phase carries as well as the total load over the entire volume comprising both matrix and fiber phases. In this study, an algorithm was developed to generate random representative volume elements (RVE) with varying volume fractions and minimum distances between fibers. The random microstructures were analyzed using finite element models (FEM) and the results compared to those for periodic microstructured RVEs in terms of the range of stress values, maximum stress, and homogenized stiffness values. Using a large number of random RVE analyses, a meaningful estimation for range and average maximum stress in the matrix phase was achieved. Results show that random microstructures exhibit a much larger range of stress values than periodic microstructures, resulting in an uneven distribution of load and distinct areas of high and low stress concentration in the matrix. It is shown that the maximum stress in the matrix phase, often responsible for failure initiation, is largely dependent on the random morphology, minimum distances between fibers, and volume fraction. Moreover, it is shown that the predicted overall load-carrying capacity of the matrix changes depending on the use of random or periodic microstructures.

Keywords:
micromechanics, representative volume element (RVE), finite element, random microstructure, stress concentration

1. Introduction

Micromechanical analysis can provide researchers with a range of information on the local and global properties of composite materials. Many studies in composite structural design

*Corresponding author: h_ghayoo@encs.concordia.ca

and analysis are done at the macrostructural level using homogenized material properties, but there are a number of macrostructural behaviours that are governed by fiber/matrix interactions and properties at the microstructural (fiber) level [1, 2]. A thorough understanding of composite fiber/matrix interactions and their underlying mechanisms is critical to understanding and predicting the macrostructural behaviour of these materials.

Figure 1 shows two examples of typical periodic and random microstructures. Micromechanical analysis is traditionally performed on a periodic (or repeating) microstructure, where there are two types of periodic microstructures commonly referred to as hexagonal and square packed. The periodic microstructure assumption confines researchers to the study of global phenomena such as global effective properties, often leading to difficulties with the accurate prediction of material properties and associated behaviour under load. Because of the irregular nature of the fiber distribution within the composite cross section, a phenomenon such as failure that is highly dependent on local morphology can not be accurately studied using ordered cross sections based on the periodic microstructure assumption.

Real composite structural morphology is very different from the repeating microstructure model and there is therefore an error associated with the use of repeating microstructures for analysis, particularly in the context of non-linear problems [3]. Microstructural morphology of composites influences the magnitudes and the distribution of stresses at the microstructural scale and ultimately dictates the overall behavior of the composite material at the macrostructural level. For this reason, irregular or random microstructures based on real composite morphologies have been adopted for the evaluation of linear and non-linear properties of composites by several researchers [4, 5, 6]. Random microstructures have also been used in the computational design of novel fibers [7].

It should also be noted that analytical approaches such as the famous Mori-Tanaka method [8, 9]] and self-consistent schemes have been successful at predicting the overall properties of composites. In addition, there exist homogenization methods that can compute second order moments of local stress [10, 11]. However, analytically predicting the range and distribution of stresses and strains, and the interactions between fibers or inclusion phase remains a challenge. In a recent study, it was shown that finite element analysis results of strain maps have a good agreement with experimental results acquired from digital image correlation (DIC). [12]. And with the computational advances of recent decades, it is affordable to analyze irregular or random microstructures and study local phenomena using finite element analysis. A significant challenge associated with the analysis of random microstructures is the generation of a representative volume element (RVE) that is a

geometrical representation of the actual microstructure [13], meaning that the RVE must be statistically equivalent to a real microstructure [14, 15]. A good geometrical representation requires that the size of the RVE be optimum; if the RVE is too small it cannot include the range of irregularities that affects stress distribution and if it is too large, it is computationally expensive.

Transverse matrix microcracking is often the first mode of failure in composite structures [16] and governs the fracture process [17, 18]. The current study is focused on the transverse cross-section where the failure and fracture initiation is dominated by matrix properties and where the distribution of fibers dictates the stress concentrations and distributions in the matrix. Random microstructures are used to study the effects of morphology and fiber distribution on stress concentrations and the maximum stresses in the matrix phase of carbon-epoxy composites.

In this study, we show that the maximum stress in the matrix is largely dependent on the random morphology of the microstructure. First, the stresses in the matrix phase for periodic and random microstructures are analyzed with a new approach using an area percentage histogram. The histogram is a method to display the results for the entirety of the matrix phase for both types of microstructure. Secondly, it is shown that it is necessary to investigate a large number of random samples to ensure the inclusiveness of the analysis for maximum stress. This is because the maximum stress in the matrix phase depends on the specific random morphology and consequently, the results of analyses for maximum stress in random RVEs leads to a range of values rather than a singular value. These values then can be used in probabilistic design optimization of macro-scale structures [19] or reliability analysis, uncertainty modeling, and life prediction of composite parts [20, 21, 22].

The results show the range and frequency of the maximum stress values vary with different types of microstructures. It is shown that both the range of values as well as the maximum stress is strongly dependent on the minimum distance between fibers. Also, the modulus properties in the transverse direction change depending on the choice of microstructural representation due to the difference in the load-carrying behavior of the matrix in the random and periodic microstructures. It is shown that the matrix phase participates less in carrying the transverse load in random microstructures compared to periodic ones.

2. Microstructural representation

Although the word random implies no biased information, random microstructures follow rules such as the minimum distance between fibers. As soon as such a rule is added

to a "random" phenomena it is no longer random, and perhaps a better term for these microstructures would be pseudo-random or irregular. For the purposes of this study, however, the term "random" is used to describe irregular microstructures and the term "periodic" for regular or repeating microstructures.

Several methods exist for the generation of random microstructures. These methods can be classified in two main categories; image-processing based and numerical generation. For the first method, an image from the cross section of the composite is acquired and the microstructure topology is generated numerically using image processing techniques [23, 24, 3, 25]. This method requires several steps (image acquisition, image processing, etc) and can be computationally expensive if a large number of different random arrangements are to be studied.

The second category involves generating the random microstructures algorithmically. The primary challenge associated with these methods is to come up with an approach where the resulting microstructure is a statistically fair representation of the actual microstructure. Statistical functions such as the nearest fiber distance distribution function of virtual and actual microstructure can be compared to find a fair RVE or *Statistically Equivalent* RVE (SERVE) [14, 26]. Random Sequential Absorption (RSA) is one of the methods used to generate random positions of fibers and particles [27, 28], and has been shown to be statistically representative [29]. Another approach used by Gusev et al. [30, 31] employs a Monte Carlo technique to generate random microstructures from perturbations of a regularly packed microstructure. A similar method based on the perturbation of regular microstructure is used in [32] to generate meso-scale random RVEs. Vaughan et al.[33] used statistical data from image processing of cross-sections to generate microstructures that are representative of actual samples. A method also is developed that starts from overlapping fibers, then by moving the fibers in several steps non-overlapping realistic RVEs were generated [34]. Another algorithm called Random Sequential Expansion (RSE) has been developed that can achieve high volume fractions [35]. Another method uses a discrete element method to create RVEs that includes fibers with non-identical radii[36, 37]. Melro et al. proposed a three-step, computationally efficient algorithm for the generation of random microstructures [38]. All the above methods have been reviewed against the criteria proposed by Swaminathan et al. [14] and can generate a SERVE for a random microstructure. Table 1 lists the available methods from the literature for the generation of random microstructures.

The approach used in this study is similar to that introduced in [38], a method that has been shown to be able to achieve high volume fractions and be statistically representa-

tive [39]. First, a series of random center points is generated where the random center point generator checks to make sure there is no overlap with other previously generated fibers. The method includes the option of defining a minimum distance between fibers. High fiber volume fractions, particularly for large $\delta = l/r$ ratios (length of RVE to radius of fiber), are not possible using the random generator alone because after a number of iterations there is no valid location for the addition of a new center point. The next step in obtaining higher fiber fractions is to move the center points in the RVE to make room for new fibers (this step is called stirring the fibers in [38]). The current work includes a novel refinement whereby the algorithm creates empty spaces by choosing the *most isolated* fibers to move. Choosing the most isolated fibers increases the probability of creating an empty space, thus increasing the chance of adding a new fiber. For example, if fibers that are already close together are moved towards each other, no empty space is created for adding a new fiber. Isolated fibers are identified by averaging the distances to three or four nearest neighbors for each fiber, and identifying isolated fibers as those with the largest average distance. The number of moving candidates can be changed depending on iteration number and desired volume fraction. Figure 2 illustrates the schematic of the isolated fiber selection method. The moving direction is towards neighboring fibers, and the move distance is a random value chosen between the determined minimum distance and the distance between two fibers. Figure 2A depicts the situation where adding a new fiber (shown with dashed lines) is not possible before moving the isolated fibers. After moving the fiber toward neighboring fibers as shown in Fig.2B, an empty space is created and the new fiber does not overlap with others.

Although the microstructure is random, the RVE itself must be periodic, meaning that if one puts a number of generated microstructures side-by-side, there will be only complete fibers in the resulting structure with no partial fibers resulting from the combination of RVEs. If a center point is close to the border of the RVE such that the distance from the border is less than the radius of the fiber, the remainder of the fiber must be repeated on the opposite side of the RVE in order to satisfy the periodicity of the RVE microstructure. The reason for the periodic RVE requirement is to permit reasonable estimates of the stress field in the RVE [3]. The use of periodic boundary conditions is explained further in Section 3.

3. Finite element implementation

The commercial Finite Element (FE) software Abaqus [40] was used to conduct this study. Random and periodic microstructures where the bonding between fibers and matrix is considered perfect are analyzed using FEM. It has been shown that interface properties

have a significant effect on failure initiation and failure path [41, 42], and damage progression and their properties are normally defined using a cohesive zone element. However, for the purpose of this study in which the material is considered to be in the elastic region, this bond is considered perfect in order to reduce the number of elements and computational time required to perform the analysis on several hundred samples.

Two types of boundary conditions (periodic and tension boundary conditions) are applied to the RVE. A large number of random microstructures were generated and values for the maximum stress in the matrix phase was extracted from each FE solution. The material properties used in this study are given in Table 2. The elements that are used are triangular 3-node linear plane strain elements. The mesh size is defined using a sensitivity analysis for different sizes of elements, and a mesh size of one fourth of the fiber radius ($r/4$) was chosen for the study.

3.1. Boundary Conditions

The boundary conditions for microstructural analysis can be applied in two ways. One approach is to embed the RVE in a homogeneous block of material where the global material properties are the same as the RVE material properties and then apply the regular displacement boundary conditions to the homogeneous block [43]. The advantage of this approach is that the RVE itself does not have to be periodic but it requires a larger number of elements and is computationally expensive. The second, more commonly employed and more efficient approach is to create a periodic or repeating RVE microstructure as discussed above where, in addition to the displacement boundary conditions, the periodic boundary conditions are also satisfied. Periodic boundary conditions (PBC) combined with repeating RVE microstructures provide an efficient tool for homogenization and microstructural analysis. In this study, the second approach (PBCs) was used for imposing boundary conditions.

Periodic boundary conditions (PBC) are imposed on the edges of the RVE. The following formulae describes the applied PBC:

$$\begin{aligned} u(0,y) - u(l_1,y) &= \varepsilon_x l_1 \\ v(x,0) - v(x,l_2) &= \varepsilon_y l_2 \end{aligned} \tag{1}$$

where u and v denote displacements, ε_x and ε_y are strains, and l_1 and l_2 are the lengths of RVE in the x and y directions, respectively. Generally, for homogenization purposes, ε_x is set equal to 1 and ε_y to 0. The effective global properties are then found by integrating the stresses over the area (or volume). A detailed description of PBCs for composites can be found in [44]. PBCs are imposed in Abaqus using the equation boundary condition option.

Figure 3 shows a typical RVE with boundary conditions, where each node at the edge of the RVE is connected with an equation (Eq. 1) to the counterpart node on the opposite edge.

While periodic boundary conditions are required to ensure the periodicity of the RVE, displacement boundary conditions are applied in order to generate stresses. For the purposes of this study, the displacement boundary conditions are applied along the x direction and are set to be equivalent to one percent strain.

Figure 4 shows a typical random RVE microstructure analyzed using the finite element model defined in this study. The reinforcement phase (fiber) is depicted as white to give an accent to the stress distributions in the matrix phase which are the focus of this study. The areas in the matrix where the fibers are close together can be seen to generate high stress concentrations.

3.2. Validation of RVE size

One of the important challenges in micromechanical studies is determining the appropriate size of the RVE, a problem that has been studied by a number of researchers [3, 14, 29, 45]. In general, the mechanical response behavior of the RVE is expected to be equivalent to that of the same materials at the macro scale in order to describe the RVE as *representative*. There are statistical descriptors based on the spatial arrangement of fibers, such as the probability density function of nearest neighbor distances, that can be compared to distributions in a real microstructure in order to determine the convergence of the RVE [14, 29]. The advantage of using the statistical descriptors is that the microstructure does not necessarily require a FEM solution for a convergence study. Alternative approaches include studying the convergence of the RVE micromechanical features such as energy density, mean von Mises stress, effective properties, or strain energy [24, 29, 33, 45].

While micromechanical analyses are traditionally performed for the purpose of determining homogenized material properties such as modulus for composite materials, they can also be used for other purposes such as damage modeling and the determination of residual stresses [7, 41, 42, 46]. The failure mechanism in composites is, in general, governed by the matrix behavior. While composite materials are used in design for their fiber-dominated properties such as high stiffness and fracture toughness, it is an important consideration that the *onset* of failure usually occurs in the matrix phase. Damage often initiates as matrix micro-cracking leading to delamination between plies, particularly under fatigue loading. Often the behavior of composites in the transverse direction (perpendicular to fibers) is not considered critical in a design process based on simple loading conditions and static

strength margins. However, stress analysis in the transverse direction can reveal important information with respect to the failure mechanisms of composites.

The current study is focused on the onset of failure and stress concentrations in the matrix phase and the effects of microstructural morphology on stress distributions at the microstructural level in composites. Failure in the matrix begins at the areas with the highest stress concentrations, and the location of these areas is highly dependent on the morphology and random distribution of fibers in the cross section as shown in Fig. 4. The accuracy of the predicted stress distribution within the RVE is related to its size in that the RVE must be large enough to include a representative variety of microstructural morphologies. The current work determines the appropriate size of RVE using a convergence study based on the maximum von Mises stress (σ_v) in the matrix phase for different δ ratios, and since the fiber radius (r) is constant, the ratio of δ is directly proportional to the RVE size. For each δ, one hundred different samples with different microstructural morphologies were analyzed using FEM to find the maximum σ_v in the matrix phase for each sample. Typical random microstructures with the same fiber volume but different values of δ are shown in Figure 5 for $V_f = 50\%$. It should be noted that the actual V_f and number of fibers are identical across all of the one hundred samples (each δ and V_f), and the difference between actual V_f in FEA samples and the target V_f is negligible and always less than one percent. The values for target and actual V_fs are shown in Table 3. Figure 6 plots the average of the maximum σ_v in the matrix phase against the RVE size over a hundred different random samples and includes the standard deviation for volume fractions of 60, 50, and 40%. It can be seen that the standard deviation reduces with increasing δ, and the required size of the RVE can be considered to have converged when there is no further change in standard deviation with change in RVE size. In this study, a value of δ equal to 40 is considered to be convergent and can therefore be considered to include all possible combinations of morphologies and random patterns. It is worth noting that Terada and co-workers [3] have also studied the convergence of maximum σ_v for a single V_f of 50%, but based their findings on the study of a single microstructure. The results of the current work are based on a convergence study conducted on 3 different fiber volumes using data from the averaged results of 100 different random morphologies as a means of ensuring the convergence of the standard deviation. Figure 6 shows that for both average and standard deviation, the convergence is reached at $\delta = 40$ which is in agreement with the results of previously published convergence studies [3, 33]. This RVE size was then used for a series of statistical and micromechanical analyses of failure initiation in the matrix phase of a typical carbon/epoxy composite.

4. Results

Random microstructures under load produce stress distribution that are very different from those of periodic or repeating microstructures under the same load. While the homogenized stiffness properties obtained using random and periodic RVE microstructures may be similar, the maximum stresses and the distribution of the stresses over the matrix and fiber phases are completely different. For example, in Figure 6 the maximum stress values predicted by the random RVE model are more than twice the values predicted by the periodic RVE model. Because failure initiation in the matrix of composite materials occurs at the locations with the high stress concentration, it can be important to accurately predict both the magnitude and location of these stresses.

4.1. Stress distributions in the matrix

Figure 7 compares the stress distributions in the matrix phase between random and periodic RVE microstructures for three different volume fractions. The histograms shown in Figure 7 use matrix stress and matrix area data acquired from one hundred samples. The stresses are created by applying one percent of tensile strain, and where the minimum distance between fibers has been set to $0.05 \times r$. The stress levels and associated areas for each element of matrix phase are extracted from the model and analysed to provide the probability of occurrence for each of the defined stress levels, which corresponds to how the stress is distributed over the volume of the matrix (V_m). For example, Fig. 7c shows that the range of stress values in the random microstructures is about four times larger than in the periodic microstructure. The reason for the higher maximum stresses in the random microstructure matrix is because the fibers can be closer together, thus creating stress concentrations. The reason for the lower values of minimum stresses in random microstructures is that, for the same volume of matrix, because of random distribution of fibers there are areas of matrix that participate less in carrying the load. Moreover, we can see that the maximum matrix stress in the random microstructure in Figure 7 is more than two times that for the periodic microstructure, which means that failure could potentially initiate at much lower loads than predicted using a periodic microstructures RVE model. The results shown in Figure 7 are the acquired results for one hundred samples, and this type of histogram provides a statistical estimation for stress concentrations that can be used for failure initiation predictions.

4.2. Minimum fiber distance

Figure 4 illustrates that the stress concentrations in the matrix phase are located where the fibers are closest together. It has been shown that minimum fiber distance has a sig-

nificant effect on stress localizations for certain loading conditions [47]. Also, the effects of minimum fiber distance, as an indicator for randomness, has been studied with respect to changes in homogenized properties of composites [48]. In this work, we take a statistical approach to quantify the effect of inter-fiber distance (see Fig. 8) on stress concentrations. Three different minimum distances are defined in the algorithm that are $0.1 \times r \approx 0.3\mu m$ and $0.05 \times r \approx 0.15\mu m$ and $0.01 \times r \approx 0.03\mu m$. A typical distribution of first neighbor distance for the three type of samples is shown in Fig. 9. In reality, the minimum distance between fibers depends largely on the specific technique used to manufacture the composite and the overall quality of the part. Defects such as resin-rich areas and voids have a substantial effect on microstructural morphology, forcing fibers to be located with little or no minimum distance. This means that the stress is not distributed evenly in the microstructure and there are areas of matrix that carry a lot of the load (where fibers are close) and areas that carry little load (resin-rich areas). This uneven distribution of load can result in lower failure loads and is one of the reasons that in industries such as aerospace, where composites are used in primary load-bearing components, there are rigorous microstructural quality controls for voids and resin-rich areas. Hojo et al. showed that, in their samples, some fibers are almost touching ($\Delta_{min} \approx 0$)[47] which means high stress concentrations and dry fibers. Also, in the study conducted by Vaughan and McCarthy [33] the minimum distance was found to be $0.5\mu m$ ($\Delta_{min} \approx 0.1r$). The effects of minimal fiber distance on composite properties such as residual stress and strength has been studied by Yang et. al [49], who showed that small fiber distances have significant effects on the failure behavior. In this work, we extend this approach to the analysis of a large number of random RVEs in order to include a large spectrum of random morphologies. As a result, this study provides a spectrum histogram of maximum matrix stresses rather than a single value, providing useful data for probabilistic-type analysis. Three minimum distances were chosen to analyze possible differences in maximum stresses in the matrix phase. Three different volume fractions of 40, 50, and 60% were used with varying values for minimum distance between fibers, and for each case of V_f and minimum distance three hundred random microstructure RVE samples were generated and analyzed and the maximum von Mises stress in matrix for each case extracted from the model.

Figure 10 shows the frequency (sample count in this case) of occurrence of maximum stresses in the matrix phase for three different minimum distances and three different volume fractions. The two main results demonstrated in this figure are the range of stress values and the magnitude of the maximum stress values. For example, for $V_f = 40\%$ shown in Fig. 10a,

and the minimum distance of $0.10r$, the maximum von Mises stress in the matrix has a range of about 45 MPa, and for the same volume fraction but a lesser minimum distance of $0.05r$ this range is increased to about 50 MPa, and finally for a minimum distance of $0.1r$ the range is further increased to 90 MPa. The increase in the range of maximum stresses shows that samples with lower minimum distance are less predictable in terms of stress localization. The other observation that can be made is that when the minimum distance is set to $0.01r$ the stress values are much higher than when the minimum distance is set to $0.1r$. For $V_f = 50\%$ in Fig. 10b the average maximum stress for $0.01r$ is about 230 MPa and for the same volume fraction but larger minimum distance of $0.1r$ the stress value reduces to 160 MPa which is about 34% lower than the average for the first set of samples. Overall, Figure 10 shows the significance of minimum distance and micromechanical quality of samples in terms of maximum von Mises stresses in the matrix and failure initiation.

4.3. Load-carrying and homogenized properties study

The RVE analysis is traditionally used for homogenization purposes in order to predict the engineering stiffness properties of composite materials.The homogenized properties of composite ($\bar{E}_{ij}$) is calculated based on the following formulae:

$$\bar{E}_{ij} = \frac{F_{ij}^m + F_{ij}^f}{A\varepsilon} \tag{2}$$

in which A is the total area of the RVE ($A = A_m + A_f$), ε is the strain that is applied to the model and F_{ij}^m and F_{ij}^f are the overall forces that the matrix and fiber phases carry respectively and are obtained by the integration of the stresses over the area of each phase (A_m & A_f):

$$\begin{aligned} F_{ij}^m &= \int_{A_m} \sigma_{ij} dA \\ F_{ij}^f &= \int_{A_f} \sigma_{ij} dA \end{aligned} \tag{3}$$

Table 4 shows the results of the homogenization study for different volume fractions and types of microstructures. It shows that the load carrying capacity of the matrix decreases for random microstructures compared to periodic microstructures. This means that while the predicted maximum stress for a random microstructure is much higher than for the periodic microstructure (see Figs. 6,7), the overall amount of the matrix participating in carrying the load decreases. This is because there are areas where the fibers are sparse and, consequently,

less load is transferred to the matrix phase. In addition, there is a significant difference in the homogenized values of the composite property $\bar{E}_2$ for the case of random microstructure compared to the case of periodic ones. $\bar{E}_2$ for random microstructures is larger than that of periodic microstructures for all three of the volume fractions studied. The difference between $\bar{E}_2$ values for a volume fraction of 40% is 6 percent and increases to about 12 percent for a volume fraction of 60%. This discrepancy demonstrates the importance of using random microstructures for the determination of homogenized properties as well as for predicting failure and other nonlinear analyses.

5. Concluding remarks

In this paper, it is shown that predicted values for stress concentrations and stress distributions in the matrix phase of a composite material are largely driven by the random microstructure of the RVE and are probabilistic phenomena. Exploration of stress concentration and failure initiation at the microscale provides useful data for damage analysis of composite materials at a larger structural scale [50]. In this study, results are obtained for a spectrum of random morphologies by analyzing a large number of random RVE samples. These results have statistically-acceptable ranges of data for failure initiation and maximum stress which can be propagated in a stochastic failure analysis of composites.

The difference between random and periodic microstructures was studied in terms of the range of stresses that the matrix phase experiences as well as the overall load that each phase carries. It was shown that, as a consequence of random microstructures, there are areas where fibers are close to each other resulting in high stress concentrations. Using several hundred FE analyses, the stress concentrations for different volume fractions and minimum distances between fibers were calculated and analysed using probability histograms. Changing the minimum distance between fibers changes the probability distribution and the average maximum stresses in the matrix phase of the random RVE samples. Larger values for minimum distance results in smaller ranges of stress values and a lower average for the maximum stress in the matrix phase of the composite RVE. The effect of minimum distance is quantified in terms of variation and frequency of maximum stress in random RVEs.

Lastly, predicted homogenized stiffness properties ($\bar{E}_2$) and the load-carrying participation of each phase (F_2^m and F_2^f) was determined for both periodic and random microstructures over a range of volume fractions. It was shown that the matrix of the random microstructure RVE participates less load-carrying than it does in periodic FEA models.

Acknowledgements

The financial contributions from the Natural Sciences and Engineering Research Council of Canada (NSERC) via the industrial chair on Automated Composites, Bell Helicopter Textron Canada Ltd., Bombardier Aerospace, and Concordia University are appreciated.

Table 1: Available methods from the literature for the generation of random microstructures/inclusion.

Name:	used/introduced in:
Random Sequential Absorption (RSA)	[28, 29]
Perturbation of Regular Packing	[30, 31, 32, 4, 37]*
Perturbation of Irregular Packing	[34]
Combined Method	[33]
Random Sequential Expansion (RSE)	[35]
RAND_uSTRU_GEN	[38, 39, 7]

*The method for perturbation may differ for different studies.

Table 2: Typical stiffness properties for epoxy matrix and carbon fibers in transverse direction.

Property	Value
E_f (MPa)	28000
ν_f	0.23
E_m (MPa)	2755
ν_m	0.34

Table 3: Target and actual obtained fiber volume fraction for three different target volume fractions and six different aspect ratios.

Target $V_f = 40\%$		Target $V_f = 50\%$		Target $V_f = 60\%$	
$\delta(l/r)$	Actual $V_f(\%)$	$\delta(l/r)$	Actual $V_f(\%)$	$\delta(l/r)$	Actual $V_f(\%)$
10.0	40.84	10.0	50.26	10.0	59.69
20.0	40.05	20.0	50.26	20.0	59.69
30.0	40.14	30.0	49.92	30.0	60.04
40.0	40.05	40.0	50.07	40.0	60.08
50.0	39.96	50.0	50.01	50.0	59.94
60.0	39.97	60.0	50.00	60.0	60.04

Table 4: Homogenized properties and portion of forces that each phase carries in transverse direction.

V_f	Microstructure	$\frac{F_2^m}{F_2}$	$\frac{F_2^f}{F_2}$	$\bar{E}_2$(GPa)
40%	Periodic	0.53	0.47	5.36
	Random	0.49	0.51	5.71
50%	Periodic	0.43	0.57	6.37
	Random	0.39	0.61	6.91
60%	Periodic	0.33	0.67	7.82
	Random	0.28	0.72	8.75

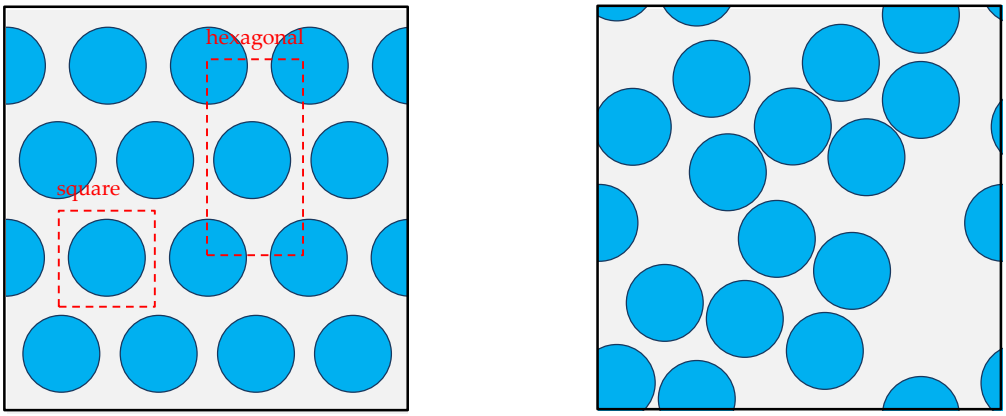

(a) Periodic microstructure (b) Random microstructure

Figure 1: Two types of microstructures with the same number of fibers (and V_f) where (a) is a periodic or uniform microstructure and (b) is a random or nonuniform microstructure. Square and hexagonal packing (or unit cells) are shown in the periodic microstructure.

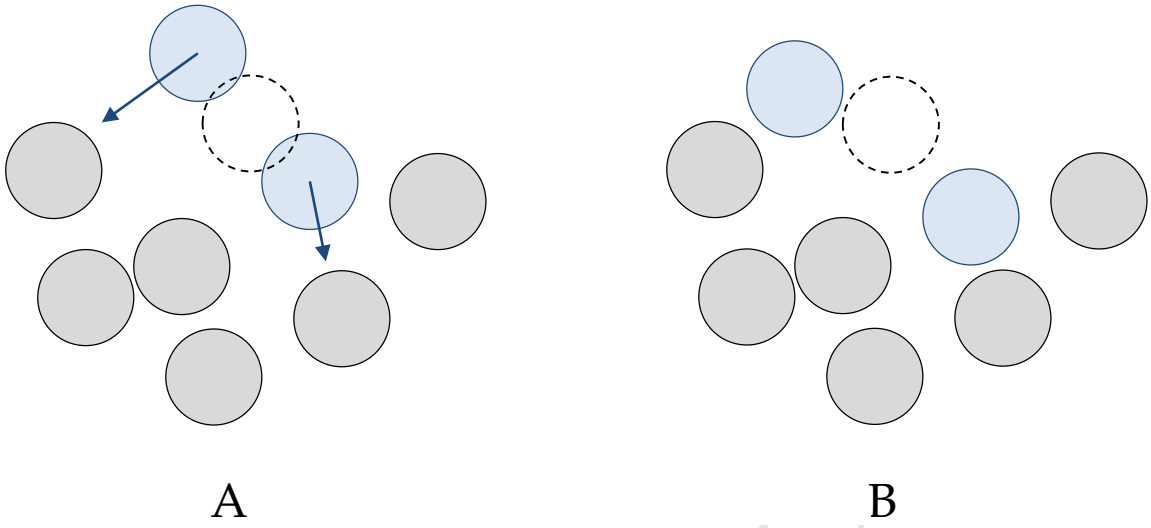

Figure 2: Schematic of moving isolated fibers. (A) shows the microstructure before moving in which adding a new fiber (dashed circle) is not possible, (B) after moving the fibers that opens a space for adding a new fiber

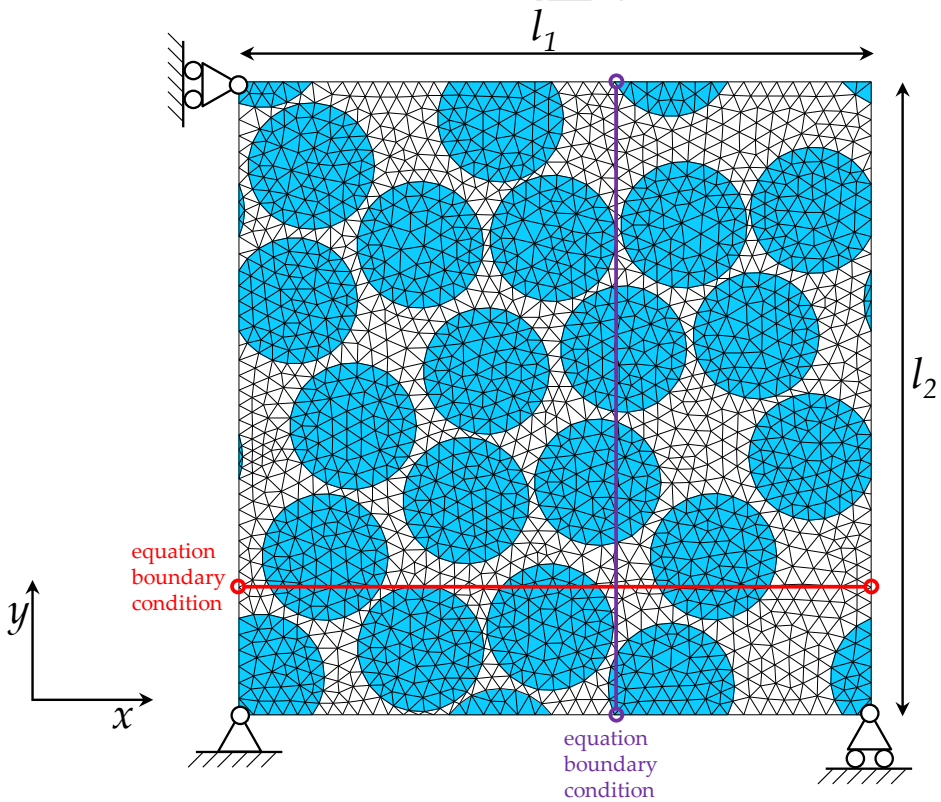

Figure 3: A typical fiber distribution in a periodic microstructure with periodic boundary conditions (PBCs). All the nodes on the edges are bound with counter nodes on the opposite edge using equation boundary conditions.

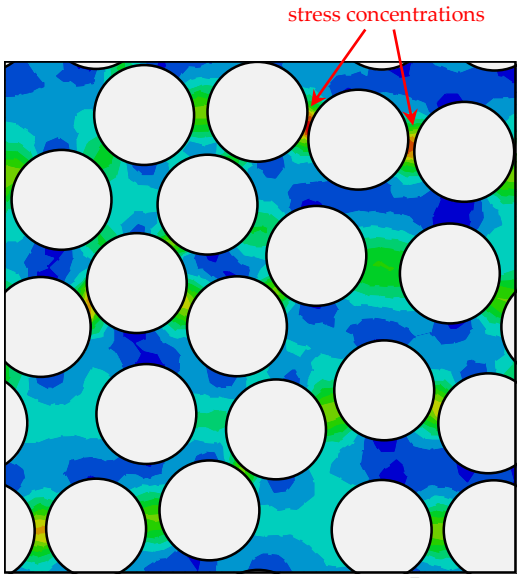

Figure 4: Stress concentrations as a result of the random morphology of a microstructure.

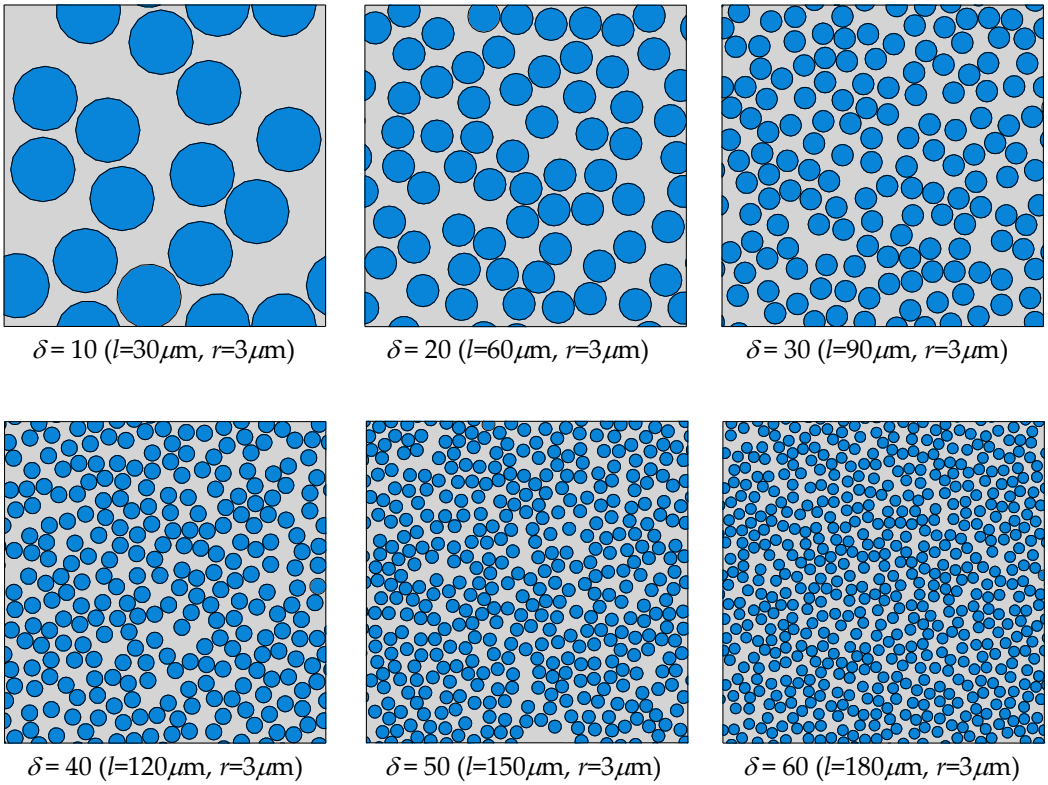

Figure 5: Typical random microstructures with $\delta = l/r$ ratios with $V_f = 50\%$.

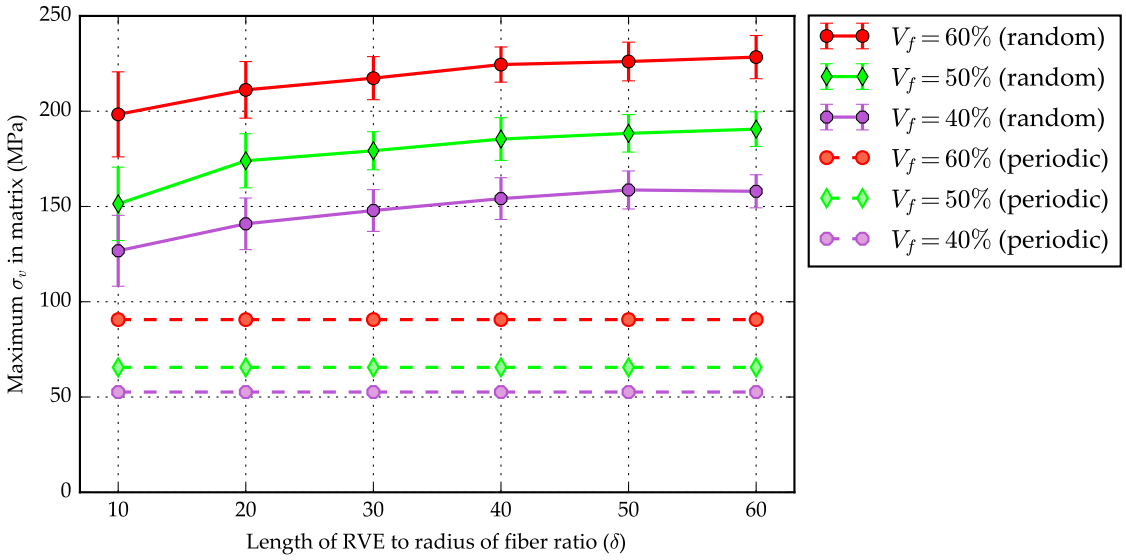

Figure 6: The average and standard deviation (error bars) of the maximum stress in the matrix for one hundred samples for both random and periodic microstructure versus to $\delta = l/r$ ratio of RVE.

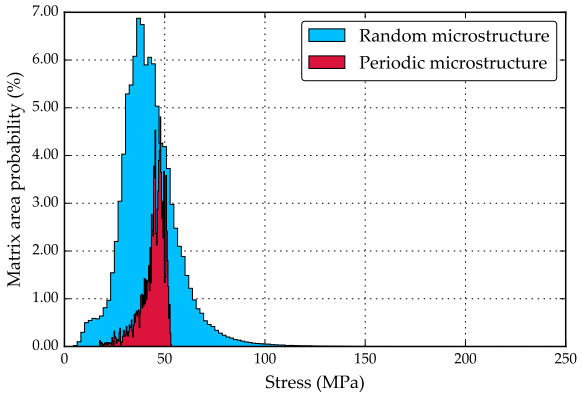

(a) V_f=40%

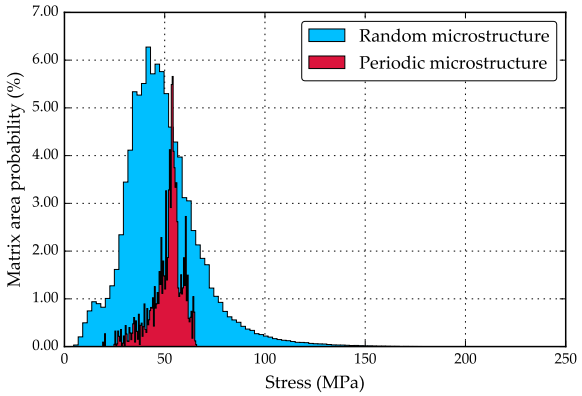

(b) V_f=50%

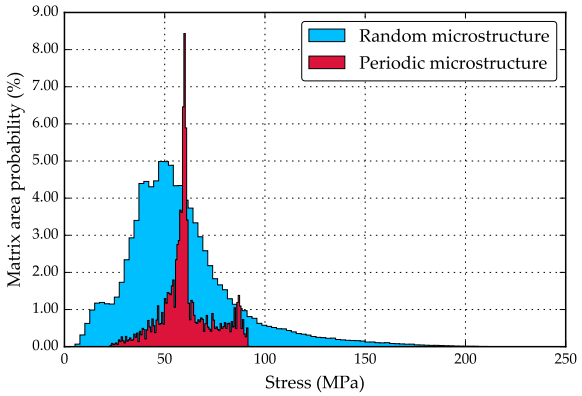

(c) V_f=60%

Figure 7: Histogram of von Mises stress in the matrix (σ_v) for volume fractions of 40, 50 and 60% for both random and periodic microstructures. The minimum distance for random microstructures are set to $0.05 \times r$. The stress is generated by applying $\varepsilon = 1\%$. The random microstructure histograms are calculated using data from one hundred samples.

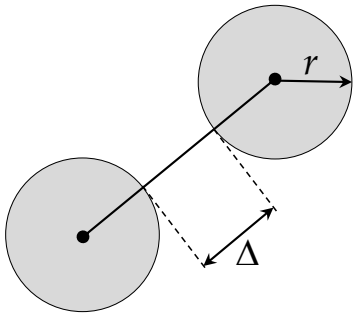

Figure 8: The distance between two fibers (inter-fiber distance) marked by Δ. The minimum distance between fibers can be altered in the algorithm.

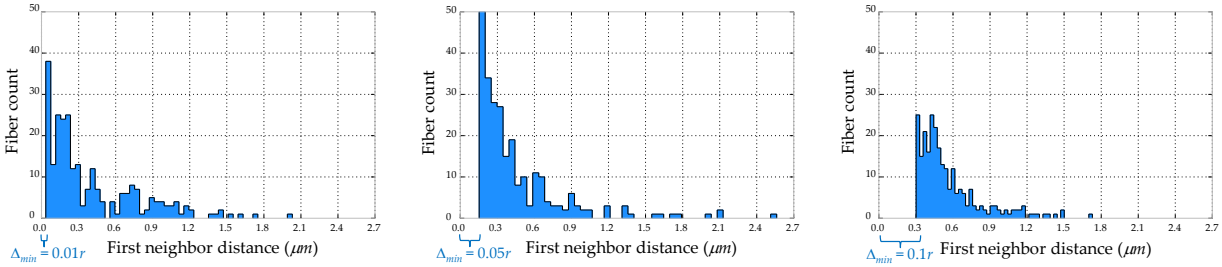

(a) Minimum distance $0.01r$ (b) Minimum distance $0.05r$ (c) Minimum distance $0.10r$

Figure 9: Typical distribution of first neighbor distance and their fiber counts for $V_f = 50\%$ and three cases of minimum distance.

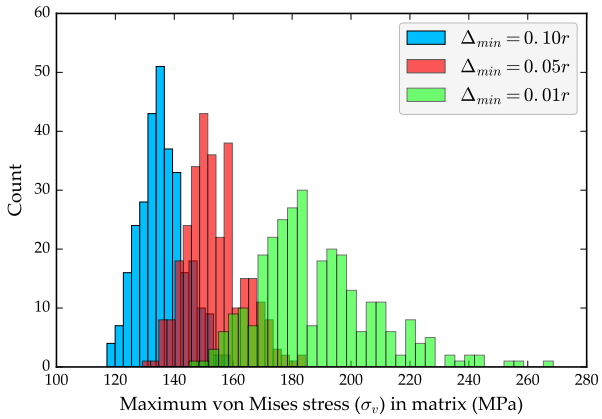

(a) V_f=40%

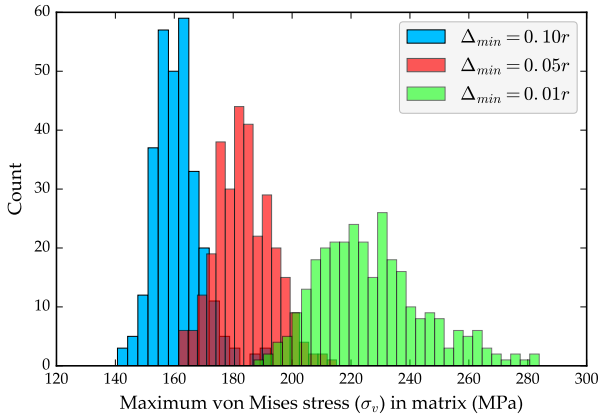

(b) V_f=50%

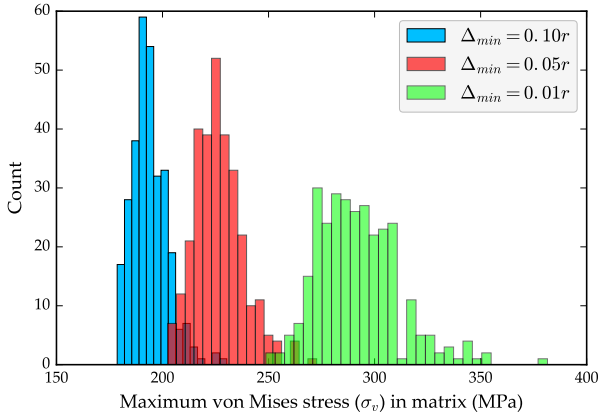

(c) V_f=60%

Figure 10: Maximum von Mises stress (σ_v) in matrix phase for three hundred random samples for each histogram.

References

[1] M. W. Hyer, Stress analysis of fiber-reinforced composite materials, DEStech Publications, Inc, 2009.

[2] J. Aboudi, Mechanics of composite materials: a unified micromechanical approach, Vol. 29, Elsevier, 2013.

[3] K. Terada, M. Hori, T. Kyoya, N. Kikuchi, Simulation of the multi-scale convergence in computational homogenization approaches, International Journal of Solids and Structures 37 (16) (2000) 2285–2311.

[4] A. Wongsto, S. Li, Micromechanical FE analysis of UD fibre-reinforced composites with fibres distributed at random over the transverse cross-section, Composites Part A: Applied Science and Manufacturing 36 (9) (2005) 1246–1266.

[5] Z. R. Khokhar, I. A. Ashcroft, V. V. Silberschmidt, Simulations of delamination in CFRP laminates: effect of microstructural randomness, Computational Materials Science 46 (3) (2009) 607–613.

[6] Y. Swolfs, R. M. McMeeking, I. Verpoest, L. Gorbatikh, Matrix cracks around fibre breaks and their effect on stress redistribution and failure development in unidirectional composites, Composites Science and Technology 108 (2015) 16–22.

[7] M. Herráez, C. González, C. Lopes, R. G. de Villoria, J. LLorca, T. Varela, J. Sánchez, Computational micromechanics evaluation of the effect of fibre shape on the transverse strength of unidirectional composites: an approach to virtual materials design, Composites Part A: Applied Science and Manufacturing 91 (2016) 484–492.

[8] T. Mori, K. Tanaka, Average stress in matrix and average elastic energy of materials with misfitting inclusions, Acta metallurgica 21 (5) (1973) 571–574.

[9] Y. Benveniste, A new approach to the application of mori-tanaka's theory in composite materials, Mechanics of materials 6 (2) (1987) 147–157.

[10] P. P. Castañeda, Exact second-order estimates for the effective mechanical properties of nonlinear composite materials, Journal of the Mechanics and Physics of Solids 44 (6) (1996) 827–862.

[11] N. Lahellec, P. Suquet, On the effective behavior of nonlinear inelastic composites: Ii: A second-order procedure, Journal of the Mechanics and Physics of Solids 55 (9) (2007) 1964–1992.

[12] M. Mehdikhani, M. Aravand, B. Sabuncuoglu, M. G. Callens, S. V. Lomov, L. Gorbatikh, Full-field strain measurements at the micro-scale in fiber-reinforced composites using digital image correlation, Composite Structures 140 (2016) 192 – 201.

[13] K. C. Liu, A. Ghoshal, Validity of random microstructures simulation in fiber-reinforced composite materials, Composites Part B: Engineering 57 (2014) 56–70.

[14] S. Swaminathan, S. Ghosh, N. Pagano, Statistically equivalent representative volume elements for unidirectional composite microstructures: Part I-without damage, Journal of Composite Materials 40 (7) (2006) 583–604.

[15] I. Gitman, H. Askes, L. Sluys, Representative volume: existence and size determination, Engineering Fracture Mechanics 74 (16) (2007) 2518–2534.

[16] R. Talreja, Damage mechanics of composite materials, Elsevier, 1994.

[17] B. Fiedler, M. Hojo, S. Ochiai, K. Schulte, M. Ochi, Finite-element modeling of initial matrix failure in cfrp under static transverse tensile load, Composites science and technology 61 (1) (2001) 95–105.

[18] Y. Ismail, D. Yang, J. Ye, A dem model for visualising damage evolution and predicting failure envelope of composite laminae under biaxial loads, Composites Part B: Engineering 102 (2016) 9–28.

[19] M. Rouhi, M. Rais-Rohani, A. Najafi, Probabilistic analysis and optimization of energy absorbing components made of nanofiber enhanced composite materials, Composite Structures 100 (2013) 144–153.

[20] M. J. Bogdanor, C. Oskay, S. B. Clay, Multiscale modeling of failure in composites under model parameter uncertainty, Computational mechanics 56 (3) (2015) 389–404.

[21] L. Wang, B. Wang, S. Wei, Y. Hong, C. Zheng, Prediction of long-term fatigue life of cfrp composite hydrogen storage vessel based on micromechanics of failure, Composites Part B: Engineering 97 (2016) 274–281.

[22] L. Wang, C. Zheng, S. Wei, Z. Wei, Micromechanics-based progressive failure analysis of carbon fiber/epoxy composite vessel under combined internal pressure and thermomechanical loading, Composites Part B: Engineering 89 (2016) 77–84.

[23] V. Buryachenko, N. Pagano, R. Kim, J. Spowart, Quantitative description and numerical simulation of random microstructures of composites and their effective elastic moduli, International Journal of Solids and Structures 40 (1) (2003) 47–72.

[24] K. Terada, T. Miura, N. Kikuchi, Digital image-based modeling applied to the homogenization analysis of composite materials, Computational Mechanics 20 (4) (1997) 331–346.

[25] D. Mortell, D. Tanner, C. McCarthy, A virtual experimental approach to microscale composites testing, Composite Structures 171 (2017) 1–9.

[26] S. H. R. Sanei, E. J. Barsotti, D. Leonhardt, R. S. Fertig, Characterization, synthetic generation, and statistical equivalence of composite microstructures, Journal of Composite Materials (2016) 1–13.

[27] J. Ohser, F. Mücklich, Statistical analysis of microstructures in materials science, Wiley, 2000.

[28] S. Kari, H. Berger, R. Rodriguez-Ramos, U. Gabbert, Computational evaluation of effective material properties of composites reinforced by randomly distributed spherical particles, Composite Structures 77 (2) (2007) 223–231.

[29] D. Trias, J. Costa, A. Turon, J. Hurtado, Determination of the critical size of a statistical representative volume element (SRVE) for carbon reinforced polymers, Acta Materialia 54 (13) (2006) 3471–3484.

[30] A. A. Gusev, P. J. Hine, I. M. Ward, Fiber packing and elastic properties of a transversely random unidirectional glass/epoxy composite, Composites Science and Technology 60 (4) (2000) 535–541.

[31] A. A. Gusev, Numerical identification of the potential of whisker-and platelet-filled polymers, Macromolecules 34 (9) (2001) 3081–3093.

[32] Z. Wang, X. Wang, J. Zhang, W. Liang, L. Zhou, Automatic generation of random distribution of fibers in long-fiber-reinforced composites and mesomechanical simulation, Materials & Design 32 (2) (2011) 885–891.

[33] T. Vaughan, C. McCarthy, A combined experimental-numerical approach for generating statistically equivalent fibre distributions for high strength laminated composite materials, Composites Science and Technology 70 (2) (2010) 291–297.

[34] M. Pathan, V. Tagarielli, S. Patsias, P. Baiz-Villafranca, A new algorithm to generate representative volume elements of composites with cylindrical or spherical fillers, Composites Part B: Engineering 110 (2017) 267–278.

[35] L. Yang, Y. Yan, Z. Ran, Y. Liu, A new method for generating random fibre distributions for fibre reinforced composites, Composites Science and Technology 76 (2013) 14–20.

[36] Y. Ismail, Y. Sheng, D. Yang, J. Ye, Discrete element modelling of unidirectional fibre-reinforced polymers under transverse tension, Composites Part B: Engineering 73 (2015) 118 – 125.

[37] Y. Ismail, D. Yang, J. Ye, Discrete element method for generating random fibre distributions in micromechanical models of fibre reinforced composite laminates, Composites Part B: Engineering 90 (2016) 485 – 492.

[38] A. Melro, P. Camanho, S. Pinho, Generation of random distribution of fibres in long-fibre reinforced composites, Composites Science and Technology 68 (9) (2008) 2092–2102.

[39] V. Romanov, S. V. Lomov, Y. Swolfs, S. Orlova, L. Gorbatikh, I. Verpoest, Statistical analysis of real and simulated fibre arrangements in unidirectional composites, Composites Science and Technology 87 (2013) 126–134.

[40] Abaqus, version 6.11 User's Manual, Pawtucket, RI, USA, 2011.

[41] A. Melro, P. Camanho, F. A. Pires, S. Pinho, Micromechanical analysis of polymer composites reinforced by unidirectional fibres: Part I–constitutive modelling, International Journal of Solids and Structures 50 (11) (2013) 1897–1905.

[42] A. Melro, P. Camanho, F. A. Pires, S. Pinho, Micromechanical analysis of polymer composites reinforced by unidirectional fibres: Part II–micromechanical analyses, International Journal of Solids and Structures 50 (11) (2013) 1906–1915.

[43] D. Trias, J. Costa, J. Mayugo, J. Hurtado, Random models versus periodic models for fibre reinforced composites, Computational materials science 38 (2) (2006) 316–324.

[44] C. Sun, R. Vaidya, Prediction of composite properties from a representative volume element, Composites Science and Technology 56 (2) (1996) 171–179.

[45] Z. Khisaeva, M. Ostoja-Starzewski, On the size of rve in finite elasticity of random composites, Journal of elasticity 85 (2) (2006) 153–173.

[46] D. Krause, A physically based micromechanical approach to model damage initiation and evolution of fiber reinforced polymers under fatigue loading conditions, Composites Part B: Engineering 87 (2016) 176–195.

[47] M. Hojo, M. Mizuno, T. Hobbiebrunken, T. Adachi, M. Tanaka, S. K. Ha, Effect of fiber array irregularities on microscopic interfacial normal stress states of transversely loaded ud-cfrp from viewpoint of failure initiation, Composites Science and Technology 69 (11) (2009) 1726–1734.

[48] M. K. Ballard, W. R. McLendon, J. D. Whitcomb, The influence of microstructure randomness on prediction of fiber properties in composites, Journal of Composite Materials 48 (29) (2014) 3605–3620.

[49] L. Yang, Y. Yan, J. Ma, B. Liu, Effects of inter-fiber spacing and thermal residual stress on transverse failure of fiber-reinforced polymer–matrix composites, Computational Materials Science 68 (2013) 255–262.

[50] S. Sriramula, M. K. Chryssanthopoulos, Quantification of uncertainty modelling in stochastic analysis of FRP composites, Composites Part A: Applied Science and Manufacturing 40 (11) (2009) 1673–1684.